euspen's 19th International Conference & Exhibition, Bilbao, ES, June 2019
www.euspen.eu

Flexure mechanism with increased dynamic performance by overconstraining using viscoelastic material

Sven klein Avink[1], Marijn Nijenhuis[1], Wilma Dierkes[2], Jacques Noordermeer[2], Dannis Brouwer[1]

[1]*Precision Engineering, Faculty of Engineering Technology, University of Twente, 7500AE Enschede, The Netherlands*
[2]*Elastomer Technology and Engineering, Faculty of Engineering Technology, University of Twente, 7500AE Enschede, The Netherlands*

m.nijenhuis@utwente.nl

Abstract
Flexure mechanisms are commonly designed to be exactly constrained to favour determinism, though at the expense of limitations on parasitic eigenfrequencies and support stiffness. This paper presents the use of viscoelastic material for providing additional stiffness without the indeterminism commonly associated with overconstraining. It is demonstrated experimentally that a custom synthesised elastomer compound can compensate for unintended misalignments without internal stress buildup, while improving the dynamic performance in terms of the first parasitic eigenfrequency. The measurements are corroborated by a nonlinear flexible multibody analysis.

Overconstrained, viscoelasticity, misalignment, exactly constrained, parallel leaf spring mechanism

1. Introduction

To ensure determinism, flexure mechanisms are typically designed exactly constrained [1–4]. This mitigates the problems of overconstrained designs: tolerances, misalignment errors and temperature gradients leading to internal forces that compromise system behaviour, repeatability and predictability. While generally avoided, overconstrained flexure mechanisms can offer better dynamic performance (i.e. higher parasitic eigenfrequencies).

To exploit these benefits and simultaneously avoid the problems of overconstrained designs, we are investigating a new class of flexure mechanisms in which overconstraints are applied by means of viscoelastic material. Since the effective stiffness of the viscoelastic material is frequency-dependent, the overconstraint is only present in a designed frequency range.

As a consequence, static loads e.g. due to misalignment errors, for which the exactly constrained behaviour is desired, hardly affect the mechanism. For dynamic loads, for which the overconstrained behaviour is desired, the effective stiffness and the first parasitic eigenfrequency are higher, improving aspects such as control bandwidth and tracking error.

In the literature, various publications on the merits and problems of overconstrained flexure mechanisms can be found. The effects of misalignments on stiffness, eigenfrequency, and buckling have been investigated for a single-overconstraint parallel flexure mechanism, a single-overconstraint cross-hinge mechanism, and a triple-overconstraint four-bar mechanism [5–7]. The potential of overconstrained mechanisms for higher performance has been investigated as an alternative design paradigm, referred to as elastic averaging [8]. To the knowledge of the authors, there are no earlier publications on the use of viscoelastic material for applying constraints in flexure mechanisms in order to mitigate problems normally associated with overconstrained designs.

In this paper, a single-overconstraint parallel flexure mechanism is used as a case study. The formulation of a custom synthesised elastomer is detailed. It has been designed for the purpose of improving the (high frequency) dynamic performance and decreasing the sensitivity to (low frequency) misalignment errors. Measurements on a dedicated demonstrator set-up with controllable misalignment show how these performance attributes vary for the exactly constrained, the conventionally overconstrained, and the viscoelastically overconstrained case. Simulations with a numerical model corroborate the measurements.

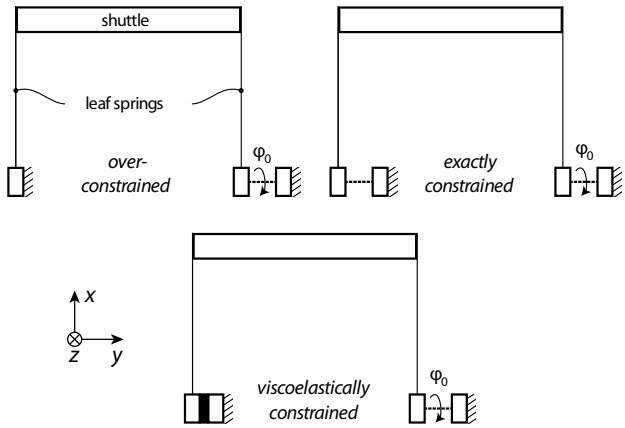

Figure 1. Schematic front view of a parallel flexure mechanism with controllable misalignment that fixes angle φ_0.

2. Methodology

2.1. Description of mechanism

A parallel flexure mechanism, consisting of two nominally identical and parallel leaf springs with a connecting shuttle, serves as the case study. This mechanism is considered to have one degree of freedom, a translation of the shuttle in the y-direction of Fig. 1, on account of the low stiffness in that direction. Motion of the shuttle in the all other directions is associated with a much higher stiffness and considered to be constrained.

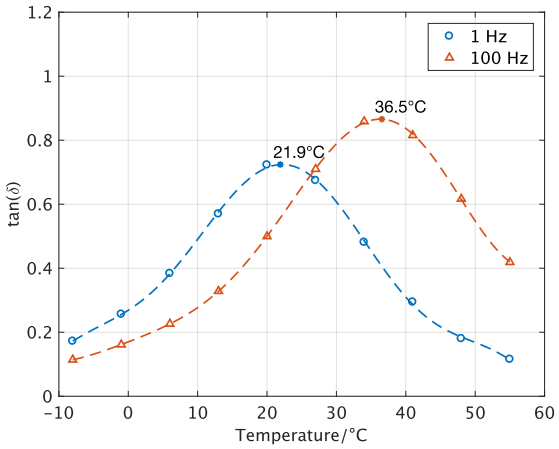

Figure 2. Glass transition temperature as indicated by tan(δ).

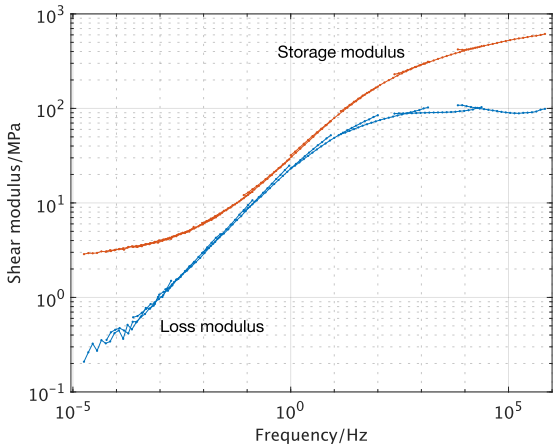

Figure 3. Shear moduli of elastomer compound at 20 degrees Celsius.

In the conventionally overconstrained case, Fig. 1, both leaf springs are clamped at the base. This way, both leaf springs constrain the rotation of the shuttle around its longitudinal axis (the rotational y-axis), leading to indeterministic behaviour, since a small misalignment angle at the base (indicated by φ_0) can induce large internal loads that affect stiffness and eigenfrequency.

In the exactly constrained case, Fig. 1, this is remedied by the use of an additional flexure hinge, which removes the redundant constraint. Only one leaf spring now constrains the longitudinal rotational motion of the shuttle about the y-axis, meaning that a misalignment angle at the base principally induces a compensating rotation of the flexure hinge, almost without any internal load and no change in system behaviour.

This particular case study has been designed to demonstrate the difference between the overconstrained and exactly constrained case. Owing to the specific location of the flexure hinge, the system's first parasitic eigenfrequency (corresponding with the second eigenfrequency) is a factor of two larger in the overconstrained case. Since this frequency typically limits the attainable bandwidth, it shows that the overconstrained system has higher dynamic performance.

In the viscoelastically constrained case, Fig. 1, a custom elastomer is placed in parallel to the flexure hinge. It allows misalignments (by providing only low stiffness) while increasing the first parasitic eigenfrequency (by providing high stiffness), on the basis of a clear distinction in the frequency range in which these two seemingly conflicting attributes are desired.

Table 1. Elastomer compound formulation.

Component	PHR
SBR	137.5
Carbon black	50
Zinc oxide	4
Stearic acid	1
TMQ	1.5
CBS	2
Sulphur	15

2.2. Elastomer compound formulation

The viscoelastic behaviour of polymers is used to apply high stiffness in only a limited frequency range. The temperature- and frequency-dependent glass transition that polymers exhibit is exploited: the rubbery state is used for misalignment compensation at low frequencies and the glassy state for a stiffness increase at high frequencies. For this application, it means that at operating temperature (20 degrees Celsius), the transition from rubber to glass should occur close before the first parasitic eigenfrequency.

Solution-polymerized styrene-butadiene rubber (S-SBR SE6233 from Sumitomo Industries, 37.5 Parts per Hundred Rubber (PHR) oil extended) is used as the base polymer in the formulation. It is a synthetic rubber with a high styrene content (40 % by mass) resulting in a glass transition temperature of -2 degrees Celsius. The material is compounded according to Table 1. With a relatively high sulphur content and long vulcanisation time of 50 minutes (increasing the cross-linking density), an even higher glass transition temperature is obtained.

The compound is characterised by means of the results from Dynamic Mechanical Analysis (DMA). Figure 2 shows the glass transition temperature for frequencies of 1 Hz and 100 Hz, as the maximum of the tan(δ) curve. It follows that at operating temperature, the compound is in the transition state at 1 Hz and in the glassy state at 100 Hz. Figure 3 shows the master curves of the shear moduli as a function of frequency for a single reference temperature of 20 degrees Celsius. The storage modulus measures the stored energy, representing the elastic portion of the material. The loss modulus measures the dissipated energy, representing the viscous portion of the material. These curves were obtained from measurements over a limited frequency range at various temperatures, in accordance with the time-temperature equivalence by using the closed-form t-T-P shifting algorithm [9].

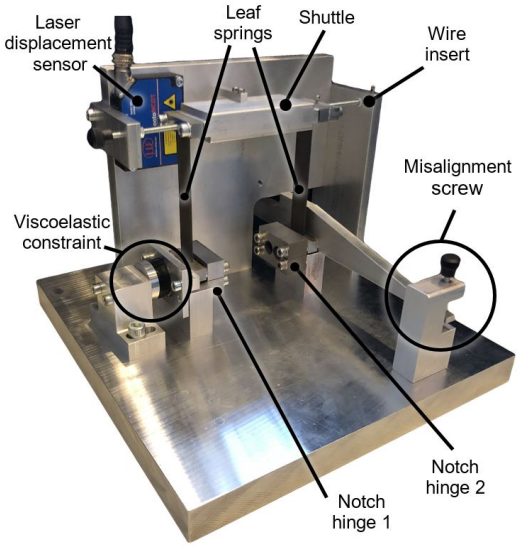

Figure 4. Experiment set-up of the parallel flexure mechanism.

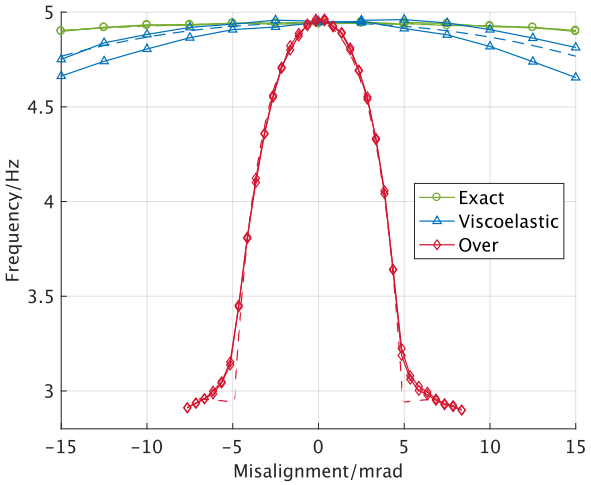

Figure 5. Measurement (solid) and simulation (dashed) of first eigenfrequency.

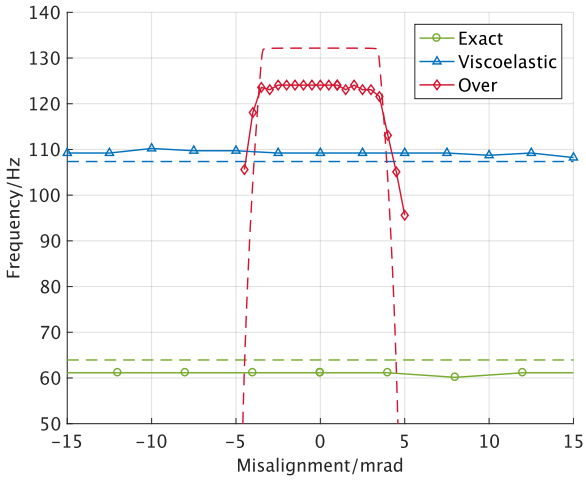

Figure 6. Measurement (solid) and simulation (dashed) of second eigenfrequency.

2.3. Experiment set-up

Figure 4 shows a photograph of the measurement set-up. It has a screw for controlling the misalignment angle and a dial gauge at the backside (not visible) for measuring the misalignment. The base plate, misalignment arm and other frame parts that carry loads are dimensioned such that parasitic compliances are negligible. The leaf springs with support fillets at the ends are made of a single piece of material (Stavax stainless steel, AISI 420) by wire EDM to avoid clamping of the leaf springs and the associated micro-slip hysteresis. The leaf springs have a nominal length of 100 mm, width of 20 mm, and thickness of 0.35 mm. Young's modulus is 200 GPa, the Poisson ratio is 0.29, and the density is 7700 kg/m³.

Notch hinge 1 serves as the flexure hinge that can remove the redundant constraint. Notch hinge 2 serves to guide the misalignment arm.

The first eigenfrequency of the system, corresponding to a mode in which the shuttle moves in its degree of freedom, serves as a measure of the misalignment sensitivity of the system, since it is affected strongly by the internal load that develops in the overconstrained case. The first eigenfrequency is measured by a laser displacement sensor.

The second eigenfrequency of the system, corresponding to a mode in which the shuttle moves in the z-direction of Fig. 1, is the performance-limiting first parasitic eigenfrequency. It is measured by accelerometers (not visible) on the shuttle. For measurement of the second eigenfrequency using modal impact testing, excessive motion of the shuttle in the degree of freedom is avoided by means of an additional wire constraint (which does not introduce any significant stiffness in the measurement direction).

2.4. Numerical model

Simulations of the system are carried out in the flexible multibody software program SPACAR. Each leaf spring is modelled by eight flexible three-dimensional beam elements that capture the linear and geometrically nonlinear effects associated with bending, shear, torsion, elongation, and warping [10,11]. The material characterisation from the DMA test is used as the constitutive relation for the elastomer compound model. A standard Kelvin-Voigt model is used with coefficients that are given by the measured storage and loss modulus as functions of frequency from Fig. 3.

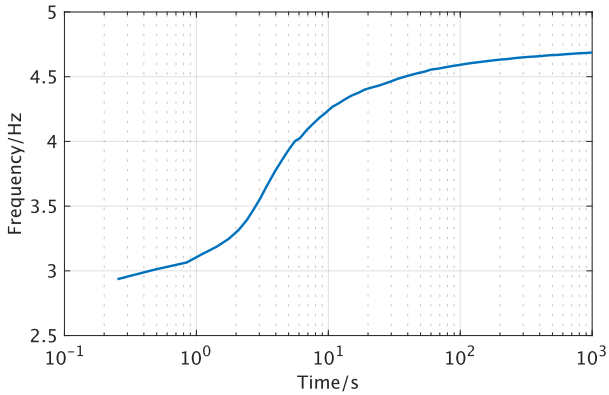

Figure 7. Measurement of the change in first eigenfrequency over time, indicating stress relaxation.

3. Results

Figure 5 shows the first eigenfrequency as a function of the misalignment angle. For all three cases, the measurement and simulation results match well. As has been reported before [5], it can be seen that the first eigenfrequency decreases strongly with misalignment in the overconstrained case. At only 5 mrad, the internal load exceeds the critical load value and bifurcation buckling occurs, indicating that stiffness is lost and the mechanism no longer functions.

In the exactly constrained case, the first eigenfrequency hardly decreases with misalignment. The small decrease that is observed in both the experiment and the simulation is due to the small but finite stiffness of the notch hinge in the set-up causing just a small internal load.

In the new viscoelastically constrained case, a minor decrease in eigenfrequency is observed, indicating the desired low sensitivity to misalignment. In the experiment, the system behaviour at the maximum possible misalignment angle of 15 mrad (three times the overconstrained value) is largely unaffected; the simulations predict a critical misalignment angle of 42 mrad.

The eigenfrequencies are measured twice: from the stress-free state of zero misalignment to maximum positive misalignment, then to maximum negative misalignment, and back to zero. Successive measurements are performed every two minutes. At the first maximum positive and negative misalignment measurement, the wait time is ten minutes; due to

stress relaxation, the frequency then increases slightly and a loop in the frequency plot is observed.

To measure the time scale at which internal stresses (caused by misalignment) decrease in the viscoelastically constrained case, a large misalignment of 15 mrad (three times the critical value of the overconstrained case) is applied quickly. Initially, this causes buckling of the mechanism. In this state, the free vibration of the shuttle, due to an excitation in the first natural mode, is recorded. The change of the first eigenfrequency over time, due to stress relaxation of the elastomer compound, is shown in Fig. 7. It can be seen that 60 % of the decrease in eigenfrequency is recovered within 10 seconds.

Figure 6 shows the second eigenfrequency as a function of the misalignment. For all three cases, the measurement and simulation results match within 6 %. It is observed that the second eigenfrequency (the first parasitic eigenfrequency) in the overconstrained case (124 Hz) is a factor of 2.03 larger than in the exactly constrained case (which is 61.1 Hz). Compared to the exactly constrained case, the new viscoelastically constrained case has an eigenfrequency of 109 Hz, which is a factor of 1.78 larger than the exactly constrained case. This clearly shows the improvement in dynamic performance over the exactly constrained case.

Also, failure of the overconstrained mechanism due to excessive misalignment can be observed: at the critical misalignment angle of 5 mrad, the second eigenfrequency drops rapidly. The viscoelastically constrained case does not show any effect of misalignment in the entire measured range.

4. Conclusion

Measurements and simulations of a demonstrator set-up of a parallel flexure mechanism with a custom synthesised elastomer compound show that

1. the first parasitic eigenfrequency goes from 61.1 Hz, without the viscoelastic overconstraint, to 109 Hz, with the viscoelastic overconstraint. This is close to the high value that can be achieved with a conventionally overconstrained design (which is 124 Hz);
2. the critical misalignment angle, at which buckling occurs and the mechanism no longer functions, goes from only 5 mrad, for the conventional overconstraint, to at least 42 mrad, for the viscoelastic overconstraint.

The measurements are corroborated by a numerical nonlinear multibody analysis combined with DMA (dynamic mechanical analysis) test results of the elastomer compound.

The results show that viscoelastic material can be used to significantly increase the dynamic performance of (flexure) mechanisms, while being tolerant to misalignments. In future work, the use of viscoelastic constraints for performance improvement in other flexure mechanisms will be investigated.

Acknowledgements

This research was funded by the Innovative Research Incentives Scheme VIDI (Stichting voor de Technische Wetenschappen) (14152 NWO TTW) of the Ministry of Education, Culture and Science of the Netherlands.

References

[1] Slocum A H 1992 *Precision Machine Design*, Englewood Cliffs, Prentice-Hall

[2] Smith S T 2000 *Flexures: Elements of Elastic Mechanisms*, CRC Press

[3] Koster M P 2000 *Constructieprincipes voor het nauwkeurig bewegen en positioneren*, Twente University Press

[4] Schellekens P, Rosielle N, Vermeulen H, Vermeulen M, Wetzels S, Pril W 1998 Design for Precision: Current Status and Trends *CIRP Annals* **47** 557-586

[5] Meijaard J P, Brouwer D M, Jonker J B 2010 Analytical and experimental investigation of a parallel leaf spring guidance *Multibody System Dynamics* **23** 77-97

[6] Van de Sande W W P J, Aarts R G K M, Brouwer D M 2015 System Behaviour of a Multiple Overconstrained Compliant Four-bar Mechanism *30thASPE Annual Meeting*, Austin, TX, USA

[7] Nijenhuis M, Brouwer D M 2016 Stiffness consequences of misalignments in an overconstrained flexure design *31stASPE Annual Meeting,* Portland, OR, USA

[8] Awtar S, Shimotsu K, Shiladitya S 2010 Elastic Averaging in Flexure Mechanisms: A Three-Beam Parallelogram Flexure Case Study *J. Mechanisms and Robotics* **2** 041006:1-12

[9] Gergesova M, Zupančič B, Saprunov I, Emri I 2011 The closed form t-T-p shifting (CFS) algorithm *J. Rheology* **55** 1-6

[10] Jonker J B, Meijaard J P 1990 SPACAR – Computer Program for Dynamic Analysis of Flexible Spatial Mechanisms and Manipulators *Multibody Systems Handbook,* Springer-Verlag, Berlin, 123-143

[11] Jonker J B, Meijaard J P 2013 A geometrically non-linear formulation of a three-dimensional beam element for solving large deflection multibody system problems *J. Non-Lin. Mechanics* **53** 63-74